

Bose-Einstein Condensate Vortices with Hypercylindrical Symmetry using Zeroth-order Dimensional Perturbation Theory

Maria Isabelle Fite

*Department of Physics and Engineering Physics,
University of Tulsa, Tulsa, Oklahoma 74104, USA.*

B. A. McKinney*

*Tandy School of Computer Science,
University of Tulsa, Tulsa, Oklahoma 74104, USA*

(Dated: November 28, 2024)

arXiv:2411.18355v1 [cond-mat.quant-gas] 27 Nov 2024

Abstract

We investigate D -dimensional atomic Bose-Einstein condensates in a hypercylindrical trap with a vortex core along the z -axis and quantized circulation $\hbar m$. We analytically approximate the hypercylindrical Gross-Pitaevskii equation using dimensional perturbation theory, where the perturbation parameter is $\delta = 1/(D + 2|m| - 3)$. We analyze lower effective dimensions due to trap anisotropy, and we compute properties of vortices in higher dimensions motivated by the study of synthetic dimensions, where additional dimensions can be simulated experimentally, and by holographic duality, where a higher-dimensional gravitational model corresponds to a lower-dimensional quantum model. We derive zeroth-order ($\delta \rightarrow 0$) semiclassical approximations for the condensate density, energy, chemical potential, and critical vortex rotation speed in arbitrary dimensions. In the zeroth-order approximation, we observe crossings between energy levels for different dimensions as a function of interaction strength and anisotropy parameters.

1. INTRODUCTION

Experimental properties of magnetically trapped Bose-Einstein condensates (BECs) of dilute atomic gases at ultra-low temperatures are well described by the mean-field nonlinear Schrodinger equation known as the Gross-Pitaevskii equation (GPE) [1]. The current study focuses on BECs in arbitrary Cartesian dimensionality, which we model using the GPE in D -dimensional hypercylindrical coordinates. We choose cylindrical coordinates because the most common anisotropic trap has axial symmetry. Using the trap anisotropy, BECs can have lower effective dimensionality, such as approximately 1D, 2D or isotropic 3D [2]. We analyze the effect of anisotropy in the cylindrical geometry as a surrogate for effective lower dimension in an isotropic system.

We also explore higher-dimensional vortex properties, which have potential applications in the emerging field of synthetic dimensions [3–5]. In these experiments, internal degrees of freedom are manipulated so that they mathematically behave like extra external degrees of freedom such as extra spatial dimensions. In another field using variable dimension, the GPE has been used to compare vortex cluster formation with predictions using a blackhole holographic model [6]. Holographic duality is a large- D result from string theory in which

* brett.mckinney@utulsa.edu

anti-de Sitter spacetimes in D spatial dimensions correspond to a conformal field theory on the boundary ($D - 1$ spatial dimensions). The focus of the current study is general- D approximations for the GPE quantum system, but the results could have applications in gravitational theory.

Previously, we used dimensional perturbation theory (DPT) to study beyond mean field effects [7], and we used the large- D limit to approximate solutions of the D -dimensional GPE [8]. In both of these cases, we assumed an isotropic BEC and hyperspherical coordinates. In the current study, we extend the large- D approximation of DPT for the isotropic GPE [8] to the anisotropic GPE with D -dimensional hypercylindrical symmetry. We use $\delta = 1/(D + 2|m| - 3)$ as our perturbation parameter, where m is the vortex quantum number, and so the zeroth-order is a large- D or large- m approximation. This approximation keeps contributions from the kinetic energy as well as keeping the full nonlinear interaction term from the GPE. We use the semiclassical approximation techniques in Ref. [9] and extend their anisotropic trap vortex collective excitation results to D dimensions. We derive semiclassical approximations of key quantities, including the condensate density, energy, chemical potential, and critical vortex speed in D dimensions. We examine the effect of D on these quantities, and we observe crossings between energy levels for different dimensions as a function of interaction strength and anisotropy parameters. We also derive the D -dimensional Thomas-Fermi approximation.

2. THE HYPERCYLINDRICAL GPE

We assume a quantized vortex of a collection of ultracold bosons, each with mass M , rotating about the z -axis in D -dimensions. This rotation results in hypercylindrical symmetry with a hyperspherical radius r_{\perp} in $(D - 1)$ Cartesian dimensions that are orthogonal to z . The time-independent GPE can then be written as

$$\left\{ -\frac{\hbar^2}{2M} \left[\frac{1}{r_{\perp}^{D-2}} \frac{\partial}{\partial r_{\perp}} \left(r_{\perp}^{D-2} \frac{\partial}{\partial r_{\perp}} \right) + \frac{\partial^2}{\partial z^2} - \frac{L_{D-2}^2}{r_{\perp}^2} \right] + \frac{1}{2} M \omega_{\perp}^2 (r_{\perp}^2 + \lambda^2 z^2) + \frac{u_D}{2} |\psi(\mathbf{r})|^2 \right\} \psi(\mathbf{r}) = \mu \psi(\mathbf{r}) \quad (1)$$

where ω_{\perp} is the confinement oscillator frequency in the hyperspherical dimension perpendicular to z and $\lambda = \frac{\omega_z}{\omega_{\perp}}$ is a measure of the anisotropy of the harmonic confinement. The hypercylindrical symmetry of the vortex fixes the L_z component of the angular momentum

to the vortex axis, and L_{D-2}^2 corresponds to the projection of the angular momentum. The eigenvalues of L_{D-2}^2 are $|m|(|m| + D - 3)$ [10], where $|m| = 0, 1, 2, \dots$. For the rotating BEC, $|m|$ is the magnitude of the projection of the angular momentum onto the z axis and the sign of m indicates the direction of rotation. $\psi(\mathbf{r})$ is the wavefunction of the condensate, normalized such that $\int |\psi(\mathbf{r})|^2 = N$, where N is the number of particles in the condensate. The role of L_{D-2}^2 is analogous to the hypercylindrical symmetry of a D -dimensional H_2^+ molecular ion [11] or hydrogen in a magnetic field [12].

The parameter u_D is the coupling constant in D dimensions, given by

$$u_D = \frac{\hbar^2}{M} \frac{2\Omega(D)}{\Gamma(D-2)} a^{D-2}, \quad (2)$$

where a is the s-wave scattering length and $\Omega(D)$ is the angular integral over a D -dimensional sphere. Because of the gamma function in the denominator, the $D = 2$ and $D = 1$ limits for u_D require careful treatment, but do exist. These limits of the pseudopotential have been calculated in Ref. [13] and Ref. [14], respectively.

Following the approach in Ref. [8], we introduce the Jacobian transformation of the wave function, $\phi = r^{(D-2)/2}\psi$, in order to eliminate the first derivatives from Eq. (1). Substituting the eigenvalues of L_{D-2}^2 then results in

$$\left\{ -\frac{\hbar^2}{2M} \left[\frac{\partial^2}{\partial r_\perp^2} + \frac{\partial^2}{\partial z^2} - \frac{(D-2)(D-4)}{4r_\perp^2} - \frac{|m|(|m| + D - 3)}{r_\perp^2} \right] + \frac{1}{2} M \omega_\perp^2 (r_\perp^2 + \lambda^2 z^2) + \frac{u_D}{2} |\psi(\mathbf{r})|^2 \right\} \phi(\mathbf{r}) = \mu \phi(\mathbf{r}), \quad (3)$$

where $a_\perp = \sqrt{\frac{\hbar}{M\omega_\perp}}$ is the oscillator length. We introduce oscillator units: $r_\perp = a_\perp \bar{r}_\perp$, $z = a_\perp \bar{z}$, $\mu = \hbar\omega_\perp \bar{\mu}$, $u_D = \hbar\omega_\perp a_\perp^D \bar{u}_D$ and $\psi(\mathbf{r}) = a_\perp^{-D/2} \bar{\psi}(\bar{\mathbf{r}})$. These transformations lead to the following hypercylindrical GPE in oscillator units:

$$\left\{ -\frac{1}{2} \left[\frac{\partial^2}{\partial \bar{r}_\perp^2} + \frac{\partial^2}{\partial \bar{z}^2} - \frac{(D-2)(D-4)}{4\bar{r}_\perp^2} - \frac{|m|(|m| + D - 3)}{\bar{r}_\perp^2} \right] + \frac{1}{2} (\bar{r}_\perp^2 + \lambda^2 \bar{z}^2) + \frac{\bar{u}_D}{2} |\bar{\psi}(\bar{\mathbf{r}})|^2 \right\} \phi(\mathbf{r}) = \bar{\mu} \phi(\mathbf{r}). \quad (4)$$

For the DPT approach, we define the perturbation parameter $\delta = 1/\kappa$, where

$$\kappa = D + 2|m| - 3, \quad (5)$$

which we use to define dimensionally scaled oscillator units: $\bar{r}_\perp = \kappa^{1/2} \hat{r}_\perp$, $\bar{z} = \kappa^{1/2} \hat{z}$, $\bar{\mu} = \kappa \hat{\mu}$, $\bar{u}_D = \kappa^{1-D} \hat{u}_D$, and $\bar{\psi}(\bar{\mathbf{r}}) = \kappa^{D/2} \hat{\psi}(\hat{\mathbf{r}})$. The dimensionally scaled GPE can then be written as

$$\left\{ -\frac{1}{2} \delta^2 \left[\frac{\partial^2}{\partial \hat{r}_\perp^2} + \frac{\partial^2}{\partial \hat{z}^2} \right] + \frac{1 - \delta^2}{8\hat{r}_\perp^2} + \frac{1}{2} (\hat{r}_\perp^2 + \lambda^2 \hat{z}^2) + \frac{\hat{u}_D}{2} |\hat{\psi}(\hat{\mathbf{r}})|^2 \right\} \phi(\mathbf{r}) = \hat{\mu} \phi(\mathbf{r}). \quad (6)$$

Note that all D and m dependence in Eq. (6) is contained in δ (or κ). The rationale behind the choice of κ is as follows. We assume $(D-4)(D-2) + 4L_{D-2}^2$ equals some polynomial in κ , with constant coefficients, and that κ is linear in $|m|$ and D . Then, κ must have the form $D + 2|m| + A$ where A is a constant. The form of L_{D-2}^2 and the factor from the Jacobian transformation in Eq. (4) means their combination is second-degree or less in m , D and κ . Using the constraint $(D-4)(D-2) + 4m(m+D-3) = \kappa^2 + b\kappa + c$, where b and c are constants not depending on D or m , we find

$$b = -2(A+3) \quad (7)$$

$$c = (A+4)(A+2). \quad (8)$$

In Ref. [8], $A = -2, -1, 0$ were used for different applications. In the current study, we let $A = -3$, so that our zeroth-order density will reduce to the $D = 3$ density in Ref. [9] (i.e., $\kappa = 2m$ for $D = 3$).

3. ZEROth ORDER (LARGE- D OR LARGE- $|m|$) APPROXIMATION

We now take the zeroth-order $\delta \rightarrow 0$ limit of Eq. (6), which can be thought of as a large- $|m|$ or large- D limit. The zeroth-order approximation of the density becomes

$$|\bar{\psi}(\bar{\mathbf{r}})|^2 \rightarrow \frac{1}{\bar{u}_D} \left(2\bar{\mu} - \bar{r}_\perp^2 - \lambda^2 \bar{z}^2 - \frac{(D+2|m|-3)^2}{4\bar{r}_\perp^2} \right), \quad (9)$$

where we reverted the dimensionally scaled oscillator (hat) units back to the more standard oscillator (bar) units. In these units, the dependence on D and $|m|$ is made explicit. Note, for $D=3$, the centrifugal term becomes $|m|^2/\bar{r}_\perp^2$ in agreement with Ref. [9]. The chemical potential is also explicitly in the zeroth-order density. Thus, to find an expression for the chemical potential $\bar{\mu}$, we use the general- D normalization condition:

$$\Omega(D-1) \iint |\bar{\psi}(\bar{\mathbf{r}})|^2 d\bar{z} \bar{r}_\perp^{D-2} d\bar{r}_\perp = N, \quad (10)$$

where $\Omega(D-1) = 2\pi^{\frac{D-1}{2}}/\Gamma(\frac{D-1}{2})$ is the angular integral corresponding to a $D-1$ dimensional sphere with $D-2$ angles. Using our zeroth-order approximation for $|\bar{\psi}(\bar{\mathbf{r}})|^2$ (Eq. 9), the integral in Eq. (10) has an exact form in terms of the hypergeometric function ${}_2F_1$ (Appendix A).

To find a simpler expression for $\bar{\mu}$ compared to Appendix A, we define a perturbation parameter

$$\alpha = (D + 2|m| - 3)/(4\bar{\mu}), \quad (11)$$

which would be the same α used in Ref. [9] if $D = 3$. We then define primed units $\bar{r}_\perp = \sqrt{2\bar{\mu}}r'_\perp$, $\bar{z} = \sqrt{2\bar{\mu}}z'$, and $|\psi'(r', z')|^2 = \frac{\Omega(D-1)}{N}|\bar{\psi}(\bar{\mathbf{r}})|^2$, which yields

$$|\bar{\psi}(r', z')|^2 = \frac{\Omega(D-1)}{N} \frac{2\bar{\mu}}{\bar{u}_D} \left(1 - r'^2_\perp - \lambda^2 z'^2 - \frac{\alpha^2}{r'^2_\perp}\right). \quad (12)$$

The z limits of integration in Eq. (10) can be found with the condition $|\bar{\psi}(\bar{\mathbf{r}}')|^2 \geq 0$:

$$z'_{max} = \frac{\sqrt{1 - r'^2_\perp - \frac{\alpha^2}{r'^2_\perp}}}{\lambda} \quad (13)$$

$$z'_{min} = -\frac{\sqrt{1 - r'^2_\perp - \frac{\alpha^2}{r'^2_\perp}}}{\lambda}. \quad (14)$$

With these substitutions and solving the z' -integral exactly, the normalization condition yields

$$\frac{4}{3\lambda} \frac{\Omega(D-1)(2\bar{\mu})^{\frac{D+2}{2}}}{\bar{u}_D} \int (1 - r'^2_\perp - \frac{\alpha^2}{r'^2_\perp})^{3/2} r'^{D-2}_\perp dr'_\perp = N. \quad (15)$$

The r'_\perp limits of integration at the edge of the condensate are then

$$r'_{\perp min} = \sqrt{\frac{1 - \sqrt{1 - 4\alpha^2}}{2}}. \quad (16)$$

$$r'_{\perp max} = \sqrt{\frac{1 + \sqrt{1 - 4\alpha^2}}{2}}. \quad (17)$$

The value $r'_{\perp min}$ is the inner radius of the condensate and can be thought of as the radius of the vortex core, while $r'_{\perp max}$ is the outer radius of the condensate. Note that $r'_{\perp min}$ and $r'_{\perp max}$ are only real for $\alpha^2 \leq \frac{1}{4}$, which yields a lower bound for the chemical potential, $\bar{\mu} \geq \kappa/2$.

Finally, expanding the normalization integrand in Eq. (15) to second order in α , we obtain an expression that can be solved numerically for the chemical potential $\bar{\mu}$:

$$\frac{4\Omega(D-1)(2\bar{\mu})^{\frac{D+2}{2}}}{3\lambda\bar{u}_D} \left[\frac{\alpha^{D-1}(D+3)}{2(D-1)(D-3)} - \frac{3\alpha^2\sqrt{\pi}\Gamma(\frac{D-1}{2})}{4(D-3)\Gamma(\frac{D}{2})} + \frac{\sqrt{\pi}\Gamma(\frac{D+1}{2})}{2(D-1)\Gamma(\frac{D+2}{2})} - \frac{\sqrt{\pi}\Gamma(\frac{D+3}{2})}{2(D+1)\Gamma(\frac{D+4}{2})} \right] \approx N. \quad (18)$$

Plotting the density (Eq. 12) requires solving Eq. (18) for $\bar{\mu}$ and restricting r_{\perp} to its lower and upper limits (Eqs. 16 and 17). As D increases, for fixed parameters N , $|m|$, λ and \bar{u}_D , the inner radius (vortex core) is pushed outward and the outer surface of the condensate is pulled inward along the r_{\perp} dimension (Fig 1). The vortex core is pushed further outward with increasing D because of the centrifugal term in the large- D density. As the interaction strength \bar{u}_D increases, the vortex radius $r'_{\perp min}$ decreases, quickly at first and then flattens (Fig. 2).

Despite the appearance of $\frac{1}{D-3}$ terms, Eq. (18) has a $D \rightarrow 3$ limit:

$$\frac{8\pi(2\bar{\mu})^{\frac{5}{2}}}{3\lambda\bar{u}_3} \left[\frac{1}{5} + \frac{3\alpha^2}{2} \left(\ln \frac{\alpha}{2} + \frac{2}{3} \right) \right] \approx N, \quad (19)$$

in agreement with Ref. [9]. Similarly, there exist limits for $D = -1, 1$. Higher-order expansions in α (beyond Eq. 18) accumulate additional poles at odd integer dimensions. The second-order expansion has no poles, while the fourth-order has a pole at $D = 3$ and the sixth-order has poles at $D = 3, 5$ (see Appendix B). For our purposes, the second-order expansion in α is a reasonable approximation, while having the advantage of a finite solution for $D = 3$. In general, we hypothesize that the n th-order expansion in α has poles at $D = 3, 5, 7, \dots, 2n-1$. So, the highest expansion possible for a given odd D , while avoiding a pole at D , is the $(D-1)$ -order expansion. There are no poles at even D regardless of the order of expansion.

Since λ , N and \bar{u}_D co-occur in Eq. (18), the $\lambda \rightarrow 0$ limit is the same as the harmonic oscillator limit $\bar{u}_D \rightarrow 0$. The solutions for these limits can be found by setting the terms in brackets of Eq. (18) equal to zero:

$$\frac{(D+3)\alpha^{D-1}}{(D-3)(D-1)} - \frac{3\sqrt{\pi}\alpha^2\Gamma\left(\frac{D-1}{2}\right)}{2(D-3)\Gamma\left(\frac{D}{2}\right)} + \sqrt{\pi} \left(\frac{\Gamma\left(\frac{D+1}{2}\right)}{(D-1)\Gamma\left(\frac{D}{2}+1\right)} - \frac{\Gamma\left(\frac{D+3}{2}\right)}{(D+1)\Gamma\left(\frac{D}{2}+2\right)} \right) = 0. \quad (20)$$

For most D , Eq. (20) involves solving a polynomial with leading order α^{D-1} , which comes from the Jacobian r'^{D-2}_{\perp} factor in the integral Eq. (15). However, for $D \rightarrow 3$, the polynomial also includes a $\ln(\alpha/2)$, which can be seen in the bracketed part of Eq. (19). Imposing the condition $\bar{\mu} \geq \kappa/2$ from Eqs. (16) and (17), Eq. (20) has a unique solution for $\bar{\mu}$.

Here we consider the effect on the zeroth order chemical potential of sweeping the parameters \bar{u}_D (interaction strength) and λ (anisotropy) for $D = 2, 3, 4, 5$. We refer to the curve of chemical potentials for a given D as the $\bar{\mu}_D$ -curve. For weak interaction strength,

the $\bar{\mu}_D$ -curves are ordered by increasing D (i.e., lower dimensions have lower chemical potential, see far left side of Fig. 3), which is expected based on the known D -dependence for the energy of a harmonic oscillator. As the interaction strength \bar{u}_D increases, $\bar{\mu}_D$ -curves cross each other, and for large interaction, the $\bar{\mu}_D$ -curves are ordered by decreasing D (i.e., higher dimensions have lower chemical potential, see right side of Fig. 3). Each $\bar{\mu}_D$ -curve crosses the others in order of D . The $\bar{\mu}_D$ -curves show the same pattern when λ anisotropy parameter is swept (Fig. 4). This similarity is because the parameters \bar{u}_D and λ play the same role in Eq. (18). The plots also include the $\bar{\mu} = \kappa/2$ (horizontal lines in Figs. 3 and 4), which come from the condition that the hyper-radii (Eqs. 17 and 16) be real ($\bar{\mu} \geq \kappa/2$). This is a lower bound on $\bar{\mu}$ that depends on the number of dimensions D and the magnitude of the angular momentum number m . As D or $|m|$ increases, the lower bound on $\bar{\mu}$ will also increase. The values of $\bar{\mu}$ stay above this lower bound even for small interactions.

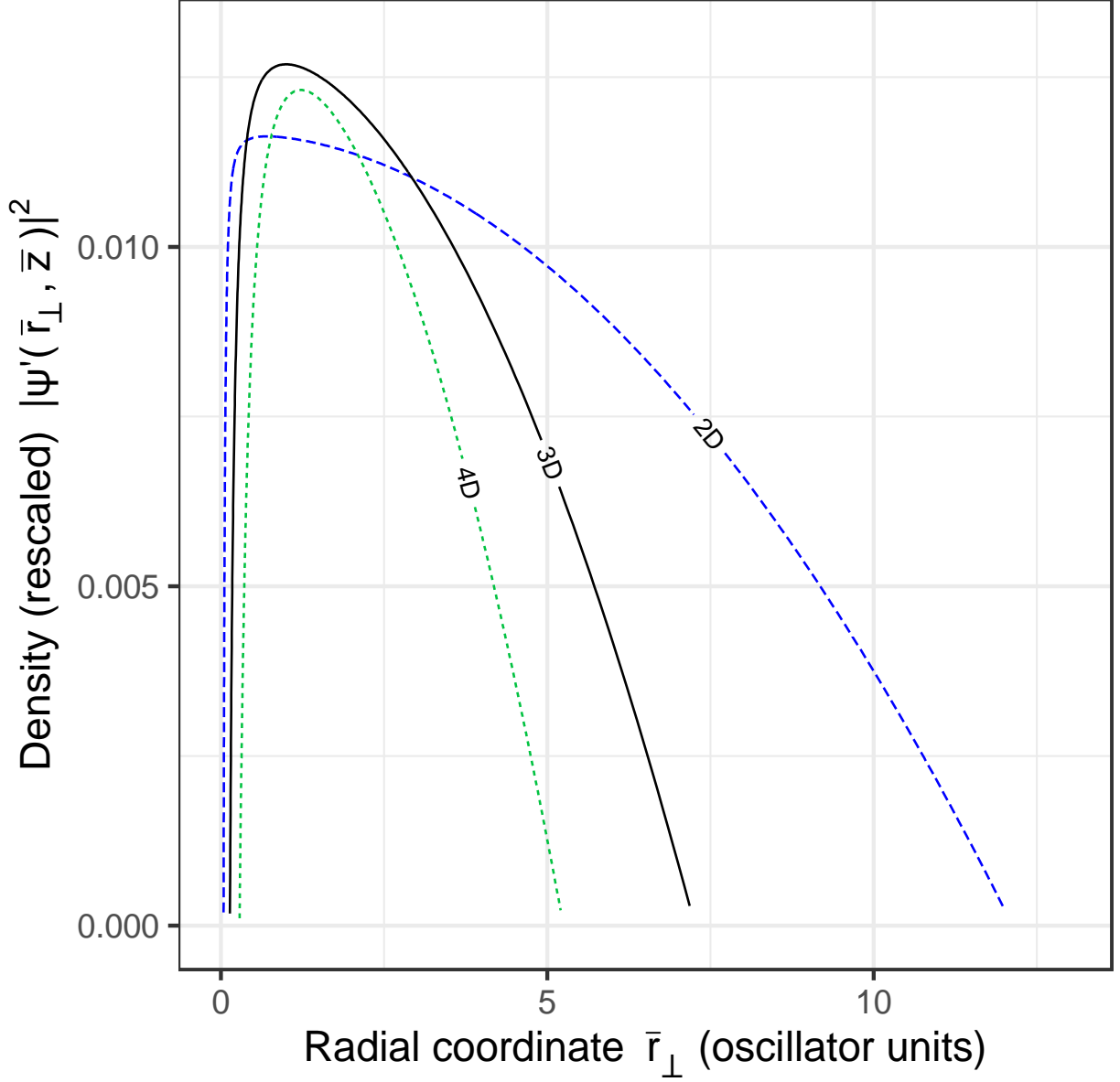


FIG. 1. Side view cross section of zeroth-order density $|\psi'(\bar{\mathbf{r}})|^2$ of Bose-Einstein condensates with different numbers of dimensions along the \bar{r}_\perp -axis, using Eqs.(9) and (18). The density $|\psi'(\bar{\mathbf{r}})|^2 = \Omega(D-1)|\bar{\psi}(\bar{\mathbf{r}})|^2/N$ is scaled so that $\iint |\psi'(\bar{\mathbf{r}})|^2 d\bar{z} \bar{r}_\perp^{D-2} d\bar{r}_\perp = 1$. We use $N = 1000$ atoms, vortex number $m = 1$, anisotropy $\lambda = 4/3$ and interaction strength $\bar{u}_D \approx 25.1$, which corresponds to scattering length $\bar{a} = 1$ in oscillator units.

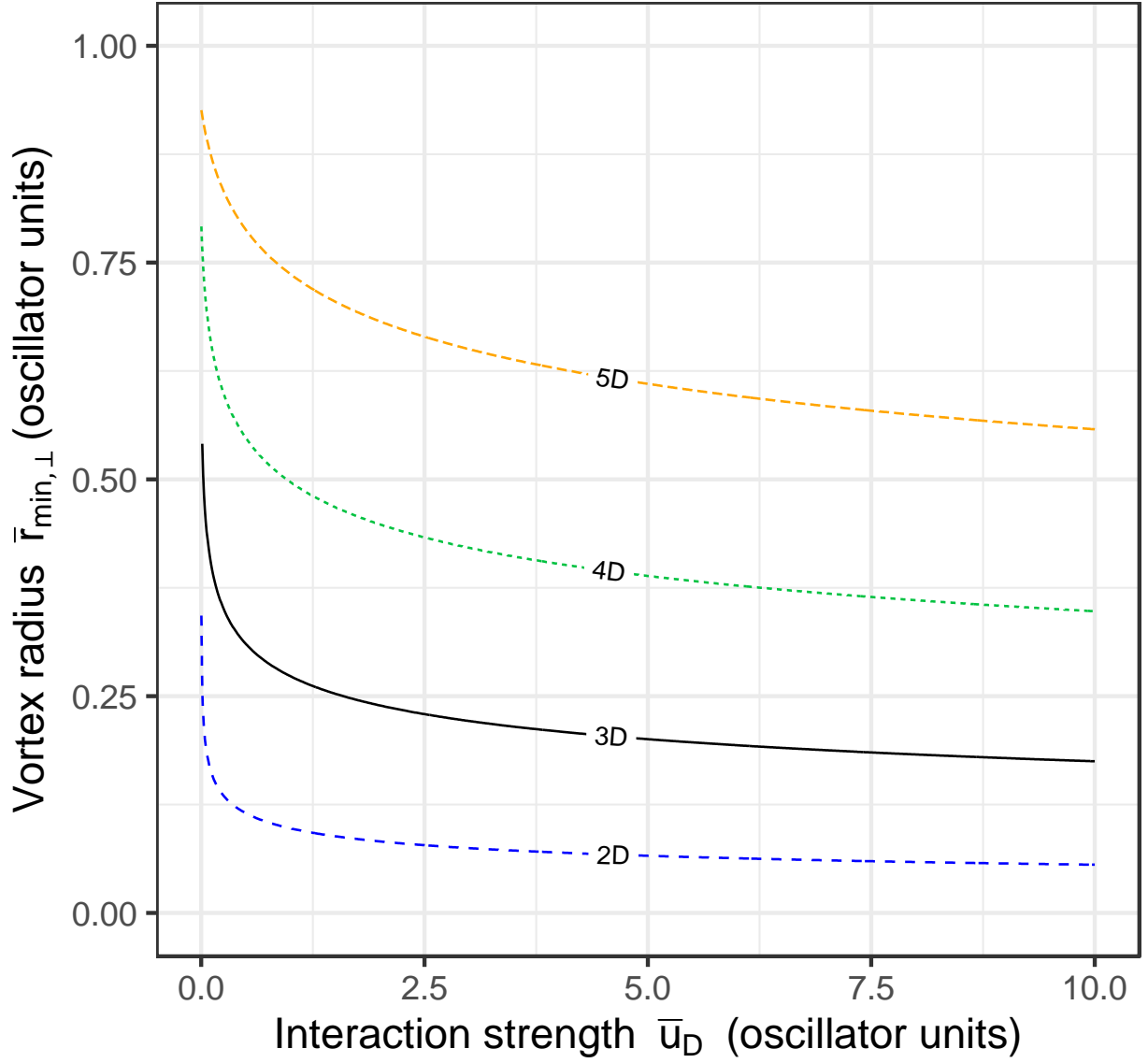


FIG. 2. Inner (vortex core) radius $r'_{\perp min}$ (from Eq. 16) as a function of the interaction strength, \bar{u}_D . We use $N = 1000$ atoms, vortex number $m = 1$, and isotropic condensates with $\lambda = 1$. The calculation includes calculation of the chemical potential $\bar{\mu}$ (Eq. 18).

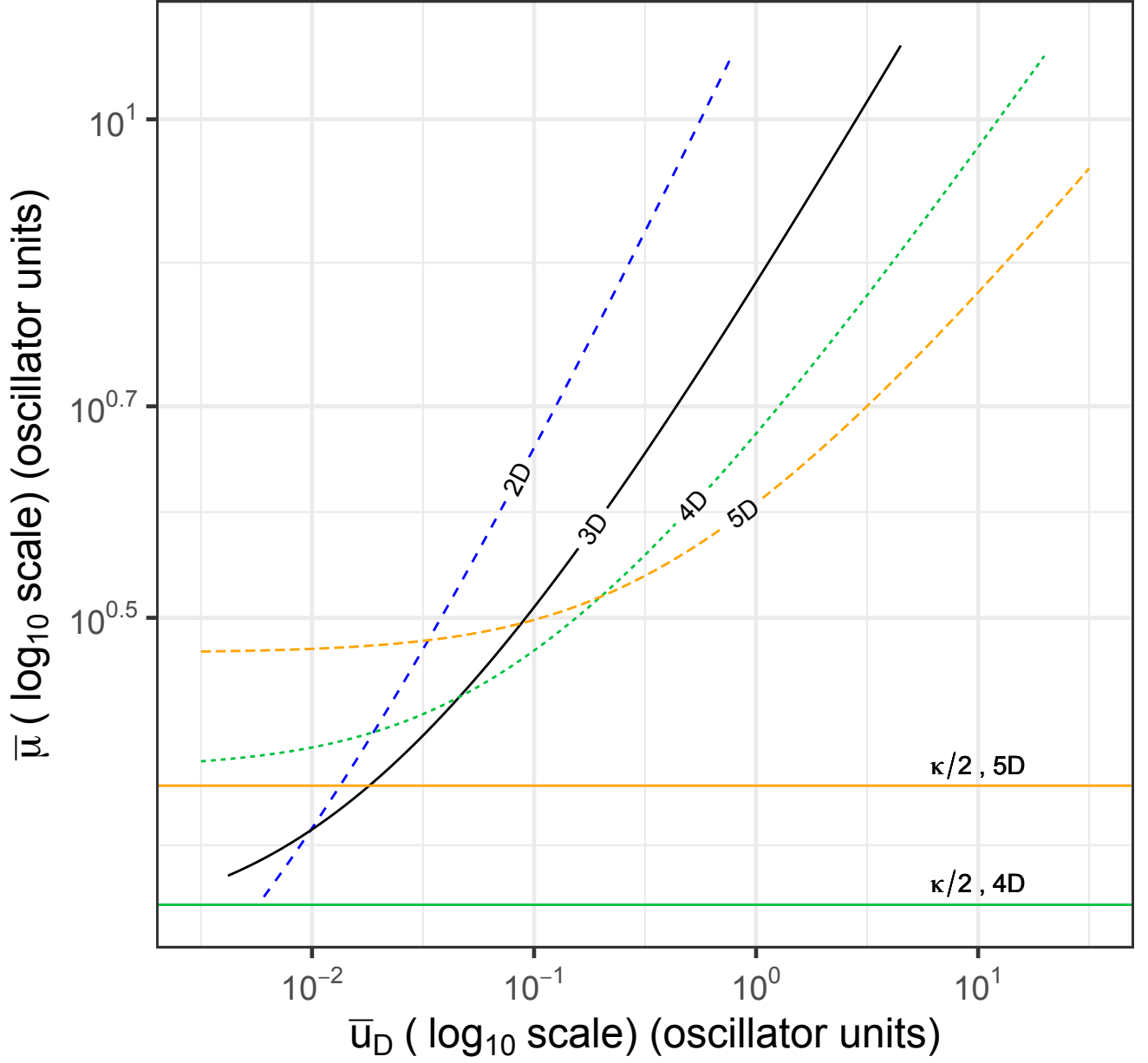


FIG. 3. Chemical potential $\bar{\mu}$ of different D dimensional condensates as a function of the interaction strength, \bar{u}_D , plotted on a log-log scale from Eq. (18). We let $N = 1000$, $m = 1$, and $\lambda = 1$. The horizontal lines are the lower bounds of the chemical potential ($\bar{\mu} = \kappa/2$) for $D = 4$ and $D = 5$.

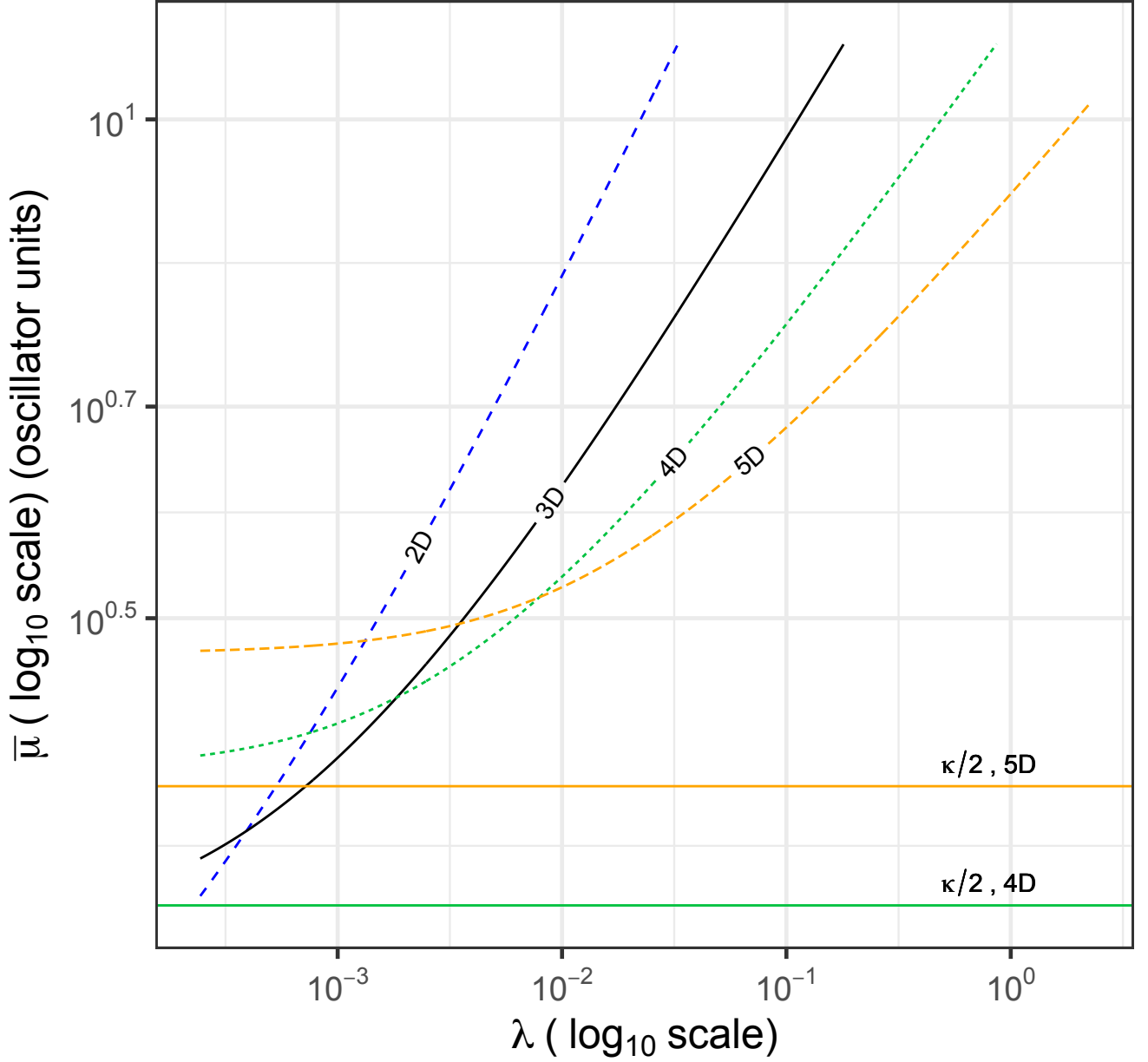


FIG. 4. Chemical potential $\bar{\mu}$ of different D dimensional condensates as a function of the trap anisotropy, λ , plotted on a log-log scale from Eq. (18). We let $N = 1000$, $m = 1$, and $\bar{u}_D = 25.1$. The horizontal lines are the lower bounds of the chemical potential ($\bar{\mu} = \kappa/2$) for $D = 4$ and $D = 5$.

Here we derive the general- D Thomas-Fermi approximation for the ground state, where the kinetic energy term is neglected completely. In the case $D = 3$, letting $|m| = 0$ in Eq.(9) yields the 3D Thomas-Fermi density

$$|\bar{\psi}(\mathbf{r})|^2 \rightarrow \frac{1}{\bar{u}_3} (2\bar{\mu} - \bar{r}_\perp^2 - \lambda^2 \bar{z}^2) \quad (21)$$

However, for $D \neq 3$ the kinetic energy contribution in Eq. (9) will be nonzero even when $|m| = 0$, because the number of dimensions contributes to the centrifugal term. Manually removing the $1/\bar{r}_\perp^2$ from Eq.(9), we analytically solve for the ground state Thomas-Fermi chemical potential $\bar{\mu}_{TF}$ using the the general- D normalization condition (Eq. 10):

$$2\bar{\mu}_{TF} = \left(\frac{(D-1)(D+2)\lambda N \bar{u}_D \Gamma(\frac{D+2}{2})}{2\sqrt{\pi}\Omega(D-1)\Gamma(\frac{D+1}{2})} \right)^{\frac{2}{D+2}}, \quad (22)$$

which matches the known result when $D = 3$ (e.g., Ref. [9]). We note that the D -dimensional Thomas-Fermi approximation forms the third term of our general- D with vortex- m implicit formula for the chemical potential (Eq. 18), which can then express in terms of the ground state Thomas-Fermi chemical potential $\bar{\mu}_{TF}$:

$$\frac{4\Omega(D-1)(2\bar{\mu})^{\frac{D+2}{2}}}{3\lambda\bar{u}_D} \left[\frac{\alpha^{D-1}(D+3)}{2(D-1)(D-3)} - \frac{3\alpha^2\sqrt{\pi}\Gamma(\frac{D-1}{2})}{4(D-3)\Gamma(\frac{D}{2})} - \frac{\sqrt{\pi}\Gamma(\frac{D+3}{2})}{2(D+1)\Gamma(\frac{D+4}{2})} \right] + \frac{N(D+2)}{3} \left(\frac{\bar{\mu}}{\bar{\mu}_{TF}} \right)^{\frac{D+2}{2}} \approx N \quad (23)$$

where recall $\alpha = \kappa/(4\bar{\mu}) = (D+2|m|-3)/(4\bar{\mu})$ contains vortex quantum number information.

4. ENERGY AND CRITICAL VELOCITY IN D DIMENSIONS: ZEROth ORDER

The general-D energy functional of the condensate is given by

$$E = \int d^D r \left(\frac{\hbar^2}{2M} |\nabla\psi(\mathbf{r})|^2 + V_{trap}(\mathbf{r})|\psi(\mathbf{r})|^2 + \frac{u_D}{4} |\psi(\mathbf{r})|^4 \right), \quad (24)$$

where $N \gg 1$, and which can be written in terms of the chemical potential:

$$\frac{\bar{E}}{N} = \bar{\mu} - \frac{\bar{u}_D}{4N} \int d^D \bar{r} |\bar{\psi}(\bar{\mathbf{r}})|^4. \quad (25)$$

Using our zeroth-order approximation for ψ in Eq.(9), and expanding the integrand of Eq.(25) to 2nd order in α , we obtain the general- D energy per particle:

$$\frac{\bar{E}}{N} \approx \bar{\mu} - \frac{(2\bar{\mu})^{\frac{D+4}{2}}\Omega(D-1)}{30\lambda N \bar{u}_D} \left[\frac{4\alpha^{D-1}(3D+1)}{(D-1)(D-3)} - \frac{15\alpha^2\sqrt{\pi}\Gamma(\frac{D-1}{2})}{(D-3)\Gamma(\frac{D+2}{2})} + \frac{6\sqrt{\pi}\Gamma(\frac{D+1}{2})}{(D-1)\Gamma(\frac{D+4}{2})} - \frac{6\sqrt{\pi}\Gamma(\frac{D+3}{2})}{(D+1)\Gamma(\frac{D+6}{2})} \right]. \quad (26)$$

Note that $\bar{\mu}$ and α depend on the vortex quantum number m . In the $D \rightarrow 3$ limit, Eq. (26) reduces to

$$\frac{\bar{E}}{N} \approx \bar{\mu} - \frac{8\pi(2\bar{\mu})^{7/2}}{15\lambda N \bar{u}_3} \left[\frac{1}{7} + \frac{5\alpha^2}{2} \left(\ln \frac{\alpha}{2} + \frac{17}{15} \right) \right], \quad (27)$$

in agreement with Ref. [9].

The energy expression in Eq. (26) allows us to approximate the critical velocity of the BEC in D dimensions. The critical angular velocity $\bar{\Omega}_c$ to produce a quantized vortex with quantum number m is

$$\bar{\Omega}_c(|m|) = \frac{1}{|m|} \left[\bar{E}(|m|)/N - \bar{E}(0)/N \right], \quad (28)$$

where $\bar{\Omega}_c$ and \bar{E}/N are in oscillator units. Substituting our energy approximation (Eq. 26) into the critical velocity equation (Eq. 28) we find

$$\begin{aligned} \bar{\Omega}_c(|m|) \approx & \frac{1}{|m|} \frac{\Omega(D-1)}{30\lambda \bar{u}_D N} \left[(2\bar{\mu}(0))^{D+4} \left(\frac{4(3D+1) \left(\frac{D-3}{4\bar{\mu}(0)} \right)^{D-1}}{(D-3)(D-1)} \right. \right. \\ & - \frac{15\sqrt{\pi} \left(\frac{D-3}{4\bar{\mu}(0)} \right)^2 \Gamma\left(\frac{D-1}{2}\right)}{(D-3)\Gamma\left(\frac{D+2}{2}\right)} + \frac{6\sqrt{\pi}\Gamma\left(\frac{D+1}{2}\right)}{(D-1)\Gamma\left(\frac{D+4}{2}\right)} - \frac{6\sqrt{\pi}\Gamma\left(\frac{D+3}{2}\right)}{(D+1)\Gamma\left(\frac{D+6}{2}\right)} \left. \right) \\ & - (2\bar{\mu}(|m|))^{D+4} \left(\frac{4(3D+1) \left(\frac{D+2|m|-3}{4\bar{\mu}(|m|)} \right)^{D-1}}{(D-3)(D-1)} - \frac{15\sqrt{\pi} \left(\frac{D+2|m|-3}{4\bar{\mu}(|m|)} \right)^2 \Gamma\left(\frac{D-1}{2}\right)}{(D-3)\Gamma\left(\frac{D+2}{2}\right)} \right. \\ & \left. \left. + \frac{6\sqrt{\pi}\Gamma\left(\frac{D+1}{2}\right)}{(D-1)\Gamma\left(\frac{D+4}{2}\right)} - \frac{6\sqrt{\pi}\Gamma\left(\frac{D+3}{2}\right)}{(D+1)\Gamma\left(\frac{D+6}{2}\right)} \right) \right] + \frac{1}{|m|} \frac{\Omega(D-1)(\bar{\mu}(|m|) - \bar{\mu}(0))}{2}, \end{aligned} \quad (29)$$

where Ω_c is the critical velocity for the vortex number m , $\bar{\mu}(0)$ is the ground-state chemical potential when $m = 0$ and $\bar{\mu}(|m|)$ is the excited-state chemical potential for the L_z quantum number. As in Eq. (26), $\lambda = \frac{\omega_z}{\omega_\perp}$ is the anisotropy parameter, \bar{u}_D is the interaction strength and N is the number of particles. For this approximation, we have expanded in $\delta = 1/\kappa = 1/(D + 2|m| - 3)$ and then expanded in α . The critical velocity is affected by the number of dimensions in the same ways as the expression for energy.

In the limit as $D \rightarrow 3$, the critical velocity becomes

$$\bar{\Omega}_c \approx \frac{|m|}{12\bar{\mu}(0)} \left[-17 + 15 \ln \frac{4\bar{\mu}(0)}{|m|} \right] + \frac{|m|}{16\bar{\mu}(0)} \left[\left(4 + 3 \ln \frac{\alpha}{4} \right) \left(7 - 15 \ln \frac{4\bar{\mu}(0)}{|m|} \right) \right] \alpha^2. \quad (30)$$

Further, for the excited vortex state, $\alpha = (D + 2|m| - 3)/(4\bar{\mu}(|m|)) \rightarrow |m|/(2\bar{\mu}(|m|))$ as $D \rightarrow 3$, and taking the limit as α goes to 0 ($\bar{\mu} \gg |m|$), the 3D critical velocity becomes

$$\bar{\Omega}_c \approx \frac{|m|}{12\bar{\mu}(0)} \left[15 \ln \frac{4\bar{\mu}(0)}{|m|} - 17 \right], \quad (31)$$

in agreement with the $D = 3$ critical velocity approximation in Ref. [9].

5. BOSE-EINSTEIN CONDENSATES IN FOUR DIMENSIONS: SYNTHETIC DIMENSIONS

BECs with $D \geq 3$ can be studied using “synthetic” dimensions, where internal degrees of freedom are used to simulate additional dimensions. Here we consider a $4D$ BEC with a vortex with hypercylindrical symmetry, where \bar{r}_\perp is the radius of a 3-dimensional sphere. Taking the limit as $D \rightarrow 4$ in Eqs. (9, 18, 26, and 28) we can estimate the density, energy, chemical potential and critical velocity of a $4D$ Bose-Einstein condensate. The density using our zeroth-order approximation becomes

$$|\bar{\psi}(\bar{\mathbf{r}})|^2 = \frac{1}{\bar{u}_4} \left(2\bar{\mu} - \bar{r}_\perp^2 - \lambda^2 \bar{z}^2 - \frac{(2|m|+1)^2}{4\bar{r}_\perp^2} \right), \quad (32)$$

where $\bar{u}_4 = 4\pi^2 a^2$ is the coupling constant parameter in 4 dimensions. The extra dimension compared to $3D$, increases the interaction strength measured by \bar{u}_d (\bar{a}^2 instead of \bar{a}), and increasing D by 1 also mimics the effect of increasing $|m|$ by $1/2$, increasing the kinetic energy contribution. In the $4D$ case, $\alpha = \kappa/(4\bar{\mu}) = (2|m|+1)/(4\bar{\mu})$ and the normalization condition becomes

$$\frac{16\pi(2\bar{\mu})^3}{3\lambda\bar{u}_4} \left[\frac{7\alpha^3}{6} - \frac{3\pi\alpha^2}{8} + \frac{\pi}{32} \right] \approx N. \quad (33)$$

The energy per particle is

$$\frac{\bar{E}}{N} \approx \bar{\mu} - \frac{2\pi(2\bar{\mu})^4}{15\lambda N\bar{u}_4} \left[\frac{52\alpha^3}{3} - \frac{15\pi\alpha^2}{4} + \frac{5\pi}{32} \right], \quad (34)$$

and the critical velocity is

$$\bar{\Omega}_c(|m|) \approx \frac{1}{20|m|} [-15\bar{\mu}(0) + (69\bar{\mu}(0) - 45\pi\bar{\mu}^2(0))x^{-1} + 2^{-2/3}15x^{1/3} - 104(2|m|+1)^3x^{-2/3} + 2^{-2/3}30(2|m|+1)^2(\frac{3\pi}{2})^{2/3}x^{-1/3}], \quad (35)$$

where the variable $x = 7 - 9\pi\bar{\mu}(0) + 12\pi\bar{\mu}^3(0) = 9\bar{u}_4\lambda N/\pi$ and $\bar{\mu}(0)$ is the $4D$ chemical potential at $m = 0$. The $\delta \rightarrow 0$ approximation is more accurate for $4D$ than $3D$, but $4D$ requires larger $\bar{\mu}$ to obtain the same accuracy in the α expansion.

6. ANISOTROPY AND LOWER EFFECTIVE ISOTROPIC DIMENSIONS

The anisotropy of a hypercylindrical condensate is governed by $\lambda = \frac{\omega_z}{\omega_\perp}$, where ω_z is the confinement oscillator frequency in the z direction and ω_\perp is the confinement oscillator frequency perpendicular to z . Our zeroth order density (Eq. 9) captures the usual condensate

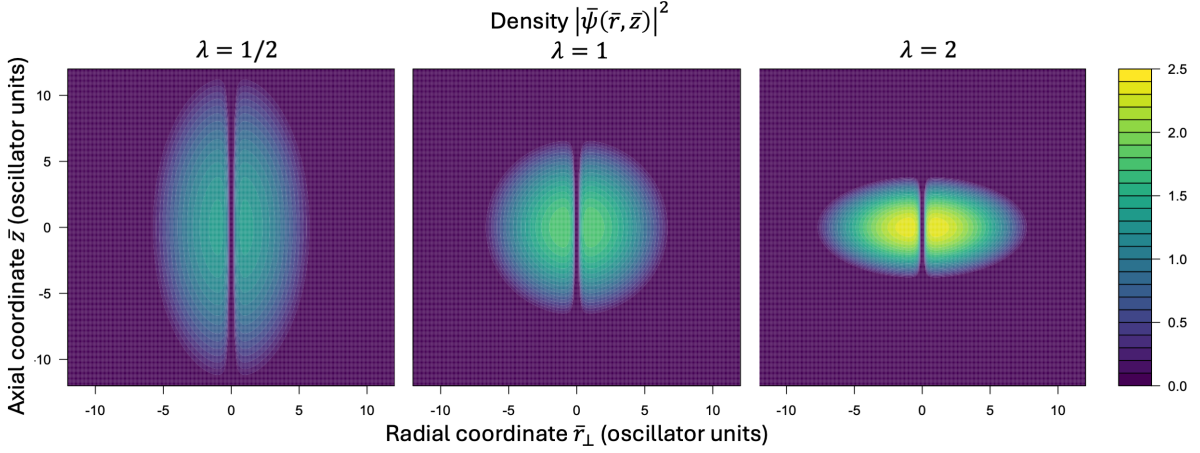


FIG. 5. Contour plots of the zeroth-order density $|\bar{\psi}(\bar{\mathbf{r}})|^2$ (Eq.9), for $D = 3$ condensates with three values of the anisotropy parameter, $\lambda = \frac{\omega_z}{\omega_\perp}$, where $\lambda \ll 1$ is the cigar and $\lambda \gg 1$ is the pancake limit. Each density is normalized such that $\iint |\bar{\psi}(\bar{\mathbf{r}})|^2 d\bar{z} \bar{r}_\perp^{D-2} d\bar{r}_\perp = N$. The coordinates \bar{r}_\perp and \bar{z} are in scaled oscillator units. The condensates have an $m = 1$ vortex along the z -axis, $N = 1000$ atoms, and interaction strength $\bar{u}_D \approx 25.1$.

features due to λ , such as stretching along the z -axis for $\lambda \ll 1$, making the BEC more 1D (cigar), while $\lambda \gg 1$ compresses along the z -axis, making the BEC a hyperpancake (Fig. 5).

We use the effect of anisotropy (λ) to find a relationship between a $D = 3$ anisotropic λ and a lower effective non-integer isotropic $D \leq 3$. A similar approach is used in [15], where the harmonic frequencies ω_x and ω_y of an external potential infinitely squeeze a quantum system through a confinement path $3D \rightarrow 2D$ or $3D \rightarrow 1D$. Because of the dominant role of z when $\lambda \gg 1$ and the spherical symmetry when $\lambda = 1$, letting λ change from 1 to ∞ represents the $3D \rightarrow 1D$ confinement path. Since the BECs we consider are hypercylindrical, we have $\omega_x = \omega_y = \omega_\perp$. We match isotropic, fractional-dimension condensates to $3D$ anisotropic condensates by their chemical potential $\bar{\mu}$ (Fig. 6).

The $2D$ case requires a different treatment. One might expect $D = 2$ to correspond to $\lambda = 0$ for a $3D$ condensate, as the z -axis becomes irrelevant, leaving two other dimensions. However, in the $3D \rightarrow 1D$ confinement path, the numerical value of λ corresponding to $D = 2$ is nonzero ($\lambda \approx 12.2$). This is due to the procedure of adjusting λ , which can be thought of as adjusting the z -axis scale. For $\lambda \gg 1$ ($D \rightarrow 1$), the BEC is stretched along z , while at $\lambda = 1$ ($D = 3$), the condensate is not stretched. In between these *lambda*'s, we find

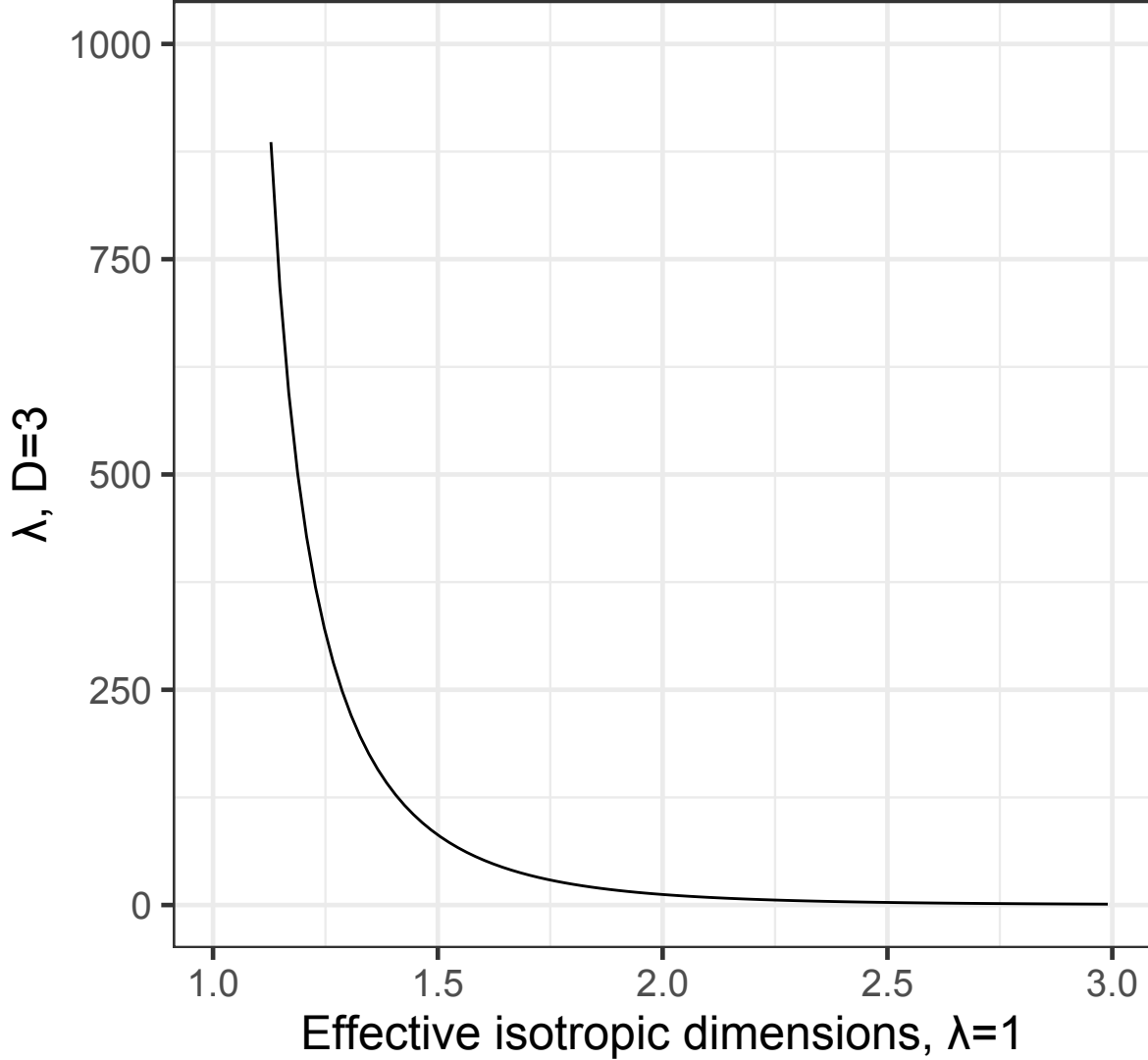


FIG. 6. Effective isotropic lower $D \leq 3$ condensates (horizontal) mapped to values of λ for 3D anisotropic condensates (vertical) by matching chemical potential $\bar{\mu}$. For instance, for $D = 1.5$ and $\lambda = 1$ (isotropic), we find $\bar{\mu}$ matches a 3D condensate with $\lambda \approx 81.4$. We use $N = 1000$, $m = 1$, and $\bar{u}_D \approx 25.1$. Note λ approaches 1 (vertical axis) for $D = 3$ (horizontal axis).

a non-zero λ that matches the chemical potential of a 2D disk but still retains some of its 3D shape. Ideally, this matching λ value would be 0. It was non-zero because the 3D \rightarrow 1D confinement path never goes through an intermediate 2D geometry. To approximate the 2D condensate, a 3D \rightarrow 2D path needs to be considered.

7. SUMMARY AND CONCLUSIONS

We used the hypercylindrical Gross-Pitaevskii equation (Eq. 1) and dimensional perturbation theory (DPT) to study vortices in D -dimensional Bose-Einstein condensates. The perturbation parameter δ involved the spatial dimension D and axial vorticity $|m|$ of the condensate. With the zeroth order, we derived semi-analytical results for arbitrary D and we studied the effect of dimensionality on the density and other properties of the condensate. For example, for higher D the density is more sharply peaked and the vortex core pushes outward (Fig. 1) due to the large- D effect of the centrifugal term. We analyzed the effect of anisotropy in the cylindrical geometry as a surrogate for effective lower dimension in an isotropic system, and we explored higher-dimensional vortex properties, which have potential applications in the emerging field of synthetic dimensions. We observe crossings between dimensions of the chemical potential curves as a function of interaction strength and anisotropy parameters.

Introducing an additional expansion in $\alpha = \kappa/(4\bar{\mu})$ (Eq. 11), we found general- D expressions for approximating the chemical potential, energy per particle, and critical vortex velocity (Eqs. 18, 26, 28). These expressions extend the results for $3D$ axially symmetric condensates in [9] to arbitrary D . In order for the inner and outer radii of the condensate to be real in $\delta \rightarrow 0$ DPT, we found a D -dependent lower bound on the chemical potential ($\bar{\mu} \geq \kappa/2$), perhaps like a D -dependent zero point energy. We also solved the normalization integral using the zeroth-order approximation without expanding in α to provide a more exact approximation for $\bar{\mu}$ (Eq. A.1). We derived the D dimensional Thomas-Fermi approximation (Eq. 22) and showed its relationship to our zeroth-order approximation for the chemical potential.

Extending the spherical symmetry in [8] to axial symmetry allowed us to study shape effects by looking at the transition between $D = 3$ and $D = 1$ as the condensate is compressed or stretched along the z -axis using λ (Fig. 6). We mapped the $3D$ condensate with varying degrees of anisotropy to the corresponding isotropic condensate with effective non-integer $D \leq 3$. We also examined the effect of D on the chemical potential as we sweep interaction strength and anisotropy, and we observe crossings between $\bar{\mu}_D$ -curves. For small interaction or anisotropy, the $\bar{\mu}_D$ -curves are ordered by increasing D (i.e., lower dimensions have lower chemical potential), and this order is reversed for large interaction or anisotropy. Each

$\bar{\mu}_D$ -curve crosses the curves in order of dimension as λ or \bar{u}_D change (Figs. 3 and 4). The locations of these crossing points and transitions between dimensions is an important area of future study.

These findings contribute to our understanding of how the chemical potential and density behave in BECs with varying dimensions, interaction strengths, vorticity and anisotropy, offering insights into the properties of lower and higher-dimensional condensates and their potential applications. We present analytical and numerical results for $D = 4$ synthetic BECs with vortices. Future work will investigate further implications of these results for synthetic BECs and for rotating black holes using holographic duality. Our DPT results involve a $D - 1$ hypersphere embedded in D dimensions analogous to a holographic duality mapping of spacetime in D spatial dimensions to a boundary in $D - 1$ spatial dimensions. Finally, an important future work will be to extend these zeroth-order results to first and higher order in δ using DPT.

Appendix A: Full zeroth-order large- κ chemical potential and energy approximations using hypergeometric functions

Instead of using an expansion in α to compute the normalization integral (Eq. 10), one can solve the integral exactly, still using the zeroth-order ψ approximation (Eq. 9). This results in a more exact normalization condition that can be solved numerically for $\bar{\mu}$:

$$\begin{aligned}
& \frac{4\Omega(D-1)(2\bar{\mu})^{\frac{D+2}{2}} i\sqrt{\pi}|\alpha|}{3\lambda \bar{u}_D 2^{\frac{D+2}{2}}}. \\
& \left[\left(\sqrt{1-4\alpha^2} + 1 \right)^{\frac{D-4}{2}} \left(\frac{4\alpha^2 \Gamma\left(\frac{D-2}{2}\right) {}_2F_1\left(-\frac{1}{2}, \frac{D-4}{2}; \frac{D-1}{2}; \frac{\sqrt{1-4\alpha^2}+1}{1-\sqrt{1-4\alpha^2}}\right)}{(D-4)\Gamma\left(\frac{D-1}{2}\right)} \right) \right. \\
& \quad + \frac{(\sqrt{1-4\alpha^2} + 1)^2 \Gamma\left(\frac{D+2}{2}\right) {}_2F_1\left(-\frac{1}{2}, \frac{D}{2}; \frac{D+3}{2}; \frac{\sqrt{1-4\alpha^2}+1}{1-\sqrt{1-4\alpha^2}}\right)}{D \Gamma\left(\frac{D+3}{2}\right)} \\
& \quad \left. - \frac{2(\sqrt{1-4\alpha^2} + 1) \Gamma\left(\frac{D}{2}\right) {}_2F_1\left(-\frac{1}{2}, \frac{D-2}{2}; \frac{D+1}{2}; \frac{\sqrt{1-4\alpha^2}+1}{1-\sqrt{1-4\alpha^2}}\right)}{(D-2)\Gamma\left(\frac{D+1}{2}\right)} \right) \\
& - \left(1 - \sqrt{1-4\alpha^2} \right)^{\frac{D-4}{2}} \left(\frac{4\alpha^2 \Gamma\left(\frac{D-2}{2}\right) {}_2F_1\left(-\frac{1}{2}, \frac{D-4}{2}; \frac{D-1}{2}; \frac{1-\sqrt{1-4\alpha^2}}{\sqrt{1-4\alpha^2}+1}\right)}{(D-4)\Gamma\left(\frac{D-1}{2}\right)} \right. \\
& \quad + \frac{(1 - \sqrt{1-4\alpha^2})^2 \Gamma\left(\frac{D+2}{2}\right) {}_2F_1\left(-\frac{1}{2}, \frac{D}{2}; \frac{D+3}{2}; \frac{1-\sqrt{1-4\alpha^2}}{\sqrt{1-4\alpha^2}+1}\right)}{D \Gamma\left(\frac{D+3}{2}\right)} \\
& \quad \left. - \frac{2(1 - \sqrt{1-4\alpha^2}) \Gamma\left(\frac{D}{2}\right) {}_2F_1\left(-\frac{1}{2}, \frac{D-2}{2}; \frac{D+1}{2}; \frac{1-\sqrt{1-4\alpha^2}}{\sqrt{1-4\alpha^2}+1}\right)}{(D-2)\Gamma\left(\frac{D+1}{2}\right)} \right) \Big] \approx N \quad (\text{A.1})
\end{aligned}$$

As before, $\Omega(D-1)$ is the angular integral over a $(D-1)$ dimensional sphere, $\lambda = \frac{\omega_z}{\omega_\perp}$ is the anisotropy parameter and N is the number of particles. Both chemical potential $\bar{\mu}$ and interaction strength \bar{u}_D are in oscillator units. The presence of $\alpha = (D + 2|m| - 3)/(4\bar{\mu})$ comes from the definition used in Eq. (12), even though here we do not expand Eq. (A.1) in α .

${}_2F_1$ is the hypergeometric function, which can be regularized using the Γ functions in the denominators to remove singularities. The quantity i is the imaginary unit, but for $0 < \alpha < 1/4$ the expression in Eq. (A.1) is real. Despite the terms $\frac{1}{D}$, $\frac{1}{D-2}$ and $\frac{1}{D-4}$ in Eq. (A.1), the limits at $D = 0, 2$ and 4 do exist.

Appendix B: Higher-order $\alpha = \kappa/(4\mu)$ expansions of the normalization condition integrand

The normalization condition in Eq. (18) uses a 2nd-order expansion in α , but higher-order expansions are possible. Since the condensate density (Eq. 12) is a function of α^2 , the odd terms in the α expansion of the normalization integrand in Eq. (15) are 0. The 4th-order alpha expansion of the normalization integrand in Eq. (15) results in the normalization condition

$$\begin{aligned} & \frac{4\Omega(D-1)(2\bar{\mu})^{\frac{D+2}{2}}}{3\bar{u}_D\lambda} \left[\frac{\alpha^{D-1}(D-9)(D+13)}{8(D-5)(D-3)(D-1)} + \frac{3\alpha^4\sqrt{\pi}\Gamma\left(\frac{D-3}{2}\right)}{8(D-5)\Gamma\left(\frac{D-4}{2}\right)} \right. \\ & \quad \left. + \frac{3\alpha^2\sqrt{\pi}}{2} \left(\frac{\Gamma\left(\frac{D+1}{2}\right)}{(D-1)\Gamma\left(\frac{D}{2}\right)} - \frac{\Gamma\left(\frac{D-1}{2}\right)}{(D-3)\Gamma\left(\frac{D-2}{2}\right)} \right) \right. \\ & \quad \left. + \sqrt{\pi} \left(\frac{\Gamma\left(\frac{D+1}{2}\right)}{(D-1)\Gamma\left(\frac{D}{2}\right)} - \frac{2\Gamma\left(\frac{D+3}{2}\right)}{(D+1)\Gamma\left(\frac{D+2}{2}\right)} + \frac{\Gamma\left(\frac{D+5}{2}\right)}{(D+3)\Gamma\left(\frac{D+4}{2}\right)} \right) \right] = N, \quad (\text{B.1}) \end{aligned}$$

where, as in Eq. (18), $\bar{\mu}$ is the chemical potential, $\lambda = \frac{\omega_z}{\omega_\perp}$ is the anisotropy parameter, \bar{u}_D is the interaction strength and N is the number of particles. The 6th-order expansion of the normalization integrand results in the normalization condition

$$\begin{aligned} & \frac{4\Omega(D-1)(2\bar{\mu})^{\frac{D+2}{2}}}{3\bar{u}_D\lambda} \left[\frac{\alpha^{D-1}(D-9)(D^2+12D-109)}{16(D-7)(D-5)(D-3)(D-1)} - \frac{\alpha^5}{80} \right. \\ & \quad - \frac{\alpha^6\sqrt{\pi}\Gamma\left(\frac{D-5}{2}\right)}{8(D-7)\Gamma\left(\frac{D-8}{2}\right)} + \frac{3\alpha^4\sqrt{\pi}}{4} \left(-\frac{\Gamma\left(\frac{D-3}{2}\right)}{(D-5)\Gamma\left(\frac{D-6}{2}\right)} + \frac{\Gamma\left(\frac{D-1}{2}\right)}{(D-3)\Gamma\left(\frac{D-4}{2}\right)} \right) \\ & \quad + 3\alpha^2\sqrt{\pi} \left(\frac{\Gamma\left(\frac{D-1}{2}\right)}{(D-3)\Gamma\left(\frac{D-4}{2}\right)} - \frac{2\Gamma\left(\frac{D+1}{2}\right)}{(D-1)\Gamma\left(\frac{D-2}{2}\right)} + \frac{\Gamma\left(\frac{D+3}{2}\right)}{(D+1)\Gamma\left(\frac{D}{2}\right)} \right) \\ & \quad + 2\sqrt{\pi} \left(-\frac{\Gamma\left(\frac{D+1}{2}\right)}{(D-1)\Gamma\left(\frac{D-2}{2}\right)} + \frac{3\Gamma\left(\frac{D+3}{2}\right)}{(D+1)\Gamma\left(\frac{D}{2}\right)} \right. \\ & \quad \left. - \frac{3\Gamma\left(\frac{D+5}{2}\right)}{(D+3)\Gamma\left(\frac{D+2}{2}\right)} + \frac{\Gamma\left(\frac{D+7}{2}\right)}{(D+5)\Gamma\left(\frac{D+4}{2}\right)} \right) \right] = N. \quad (\text{B.2}) \end{aligned}$$

Note the fourth order (Eq. B.1) approximation has a pole at $D = 3$ and so the second order approximation is more appropriate for $D = 3$. However, the fourth order approximation has a limit for $D = 5$. Similarly, the sixth order (Eq. B.2) approximation has poles at $D = 3, 5$ and a limit for $D = 7$. For Eq. (B.1) and Eq. (B.2), the $D = 1$ limit exists because of the $\Gamma((D-1)/2)$ in $\Omega(D-1)$.

REFERENCES

- [1] A. L. Fetter and A. A. Svidzinsky, *Journal of Physics: Condensed Matter* **13**, R135 (2001).
- [2] A. Görlitz, J. M. Vogels, A. E. Leanhardt, C. Raman, T. L. Gustavson, J. R. Abo-Shaeer, A. P. Chikkatur, S. Gupta, S. Inouye, T. Rosenband, and W. Ketterle, *Phys. Rev. Lett.* **87**, 130402 (2001).
- [3] B. McCanna and H. M. Price, *Phys. Rev. Res.* **3**, 023105 (2021).
- [4] O. Boada, A. Celi, J. I. Latorre, and M. Lewenstein, *Phys. Rev. Lett.* **108**, 133001 (2012).
- [5] S. Sugawa, F. Salces-Carcoba, A. R. Perry, Y. Yue, and I. B. Spielman, *Science* **360**, 1429 (2018).
- [6] W.-C. Yang, C.-Y. Xia, Y. Tian, M. Tsubota, and H.-B. Zeng, “Emergence of Large-Scale Structures in Holographic Superfluid Turbulence,” (2024), arXiv:2402.17980 [hep-th].
- [7] B. A. McKinney, M. Dunn, and D. K. Watson, *Phys. Rev. A* **69**, 053611 (2004).
- [8] B. A. McKinney and D. K. Watson, *Phys. Rev. A* **65**, 33604 (2002).
- [9] S. Sinha, *Phys. Rev. A* **55** (1997).
- [10] D. D. Frantz and D. R. Herschbach, *The Journal of Chemical Physics* **92**, 6668 (1990).
- [11] D. R. Herschbach, *Journal of Chemical Physics* **84**, 838 (1986).
- [12] G. Baym and C. J. Pethick, *Phys. Rev. Lett.* **76**, 6 (1996).
- [13] L. G. McKinney and B. A. McKinney, *Physica Scripta* **98**, 015404 (2023).
- [14] T. T. Le, Z. Osman, D. Watson, M. Dunn, and B. A. McKinney, *Physica Scripta* **94**, 065203 (2019).
- [15] E. Garrido and A. S. Jensen, *Phys. Rev. Res.* **1**, 023009 (2019).